

HYBRID ELECTROMAGNETIC SYSTEM FOR ACCELERATION OF SOLIDS

A. A. Sivkov

UDC 537.523.5

The electroexplosive and electrothermal mechanisms and the principles of conduction and induction electrodynamics are used simultaneously to convert electromagnetic energy to the kinetic energy of projectiles. This approach is implemented on the basis of the well-known configuration of a coaxial pinch accelerator. It is established that there is an “active” lengths of the barrel on which the system ensures launching with nearly constant acceleration. For a barrel length of 340 mm and a barrel diameter of 17 mm, bodies with a mass of 1–12 g are accelerated to velocities of 3.4–1.45 km/sec with an energy conversion efficiency of 25–29% at a capacitive storage voltage of 1.75 kV and a discharge current of up to 150 kA. Bodies with a mass of 40–80 g (barrel diameter 25 mm) are accelerated to velocities of 1.3–1.0 km/sec with an efficiency of 28–20% at a voltage of 3.5 kV and a current of up to 220 kA.

Experimental studies were performed on a hybrid electromagnetic accelerating system [1] powered by a capacitive storage. A diagram of this system and the replaceable unit (coaxial pinch accelerator) is presented in Fig. 1. The main elements of the accelerator, the central electrode and the barrel electrode in the initial state are connected by electrically exploding conductors. The accelerator electrodes are fixed hermetically by means of an insulator and a steel housing. The projectile is installed at the top of the central electrode at the beginning of the barrel. The main element of the stationary part of the system is a powerful inductor solenoid. The central electrode of the accelerator is electrically connected to an auxiliary disk electrode, which is pressed to the edge of the barrel. Between the disk electrode and the barrel edge there is an insulation ring 10 mm thick. The auxiliary electrode is intended for shunting of the pinch accelerator when the projectile leaves the barrel and for closure of the gap by a plasma. In the simplest circuit, the inductor and the pinch accelerator are powered by the same electric power supply C . The switch S causes the capacitive storage to carry the load at time $t = 0$. For a certain value of the current strength at time t_1 , an electric explosion of the conductors occurs. The projectile gains an initial momentum, and the accelerator then begins to work.

Optimization of the electroexplosive effect allows one to attain rather large initial velocities [2] but with a low efficiency of conversion of the input energy (2–3%). Therefore, at the initial moment, it is expedient to produce conditions for fast operation of the electrothermal mechanism with simultaneous formation of a high-current discharge plasma structure of the Z -pinch type. This plasma configuration is produced by a cylindrical channel in a polymeric insulator along which several copper conductors run and then radiate symmetrically to the wall of the barrel channel [3]. The plasma structure formed consists of a plasma cord (pinch) and a plasma bridge (armature). Immediate contact between the discharge plasma with a current of 10^4 – 10^5 A and the channel wall causes intense ablation and thermal decomposition of the polymeric dielectric (for example, polyethylene). This simple electrothermal mechanism of energy conversion has attracted the attention of the majority of scientists working with pinch accelerators [4–6].

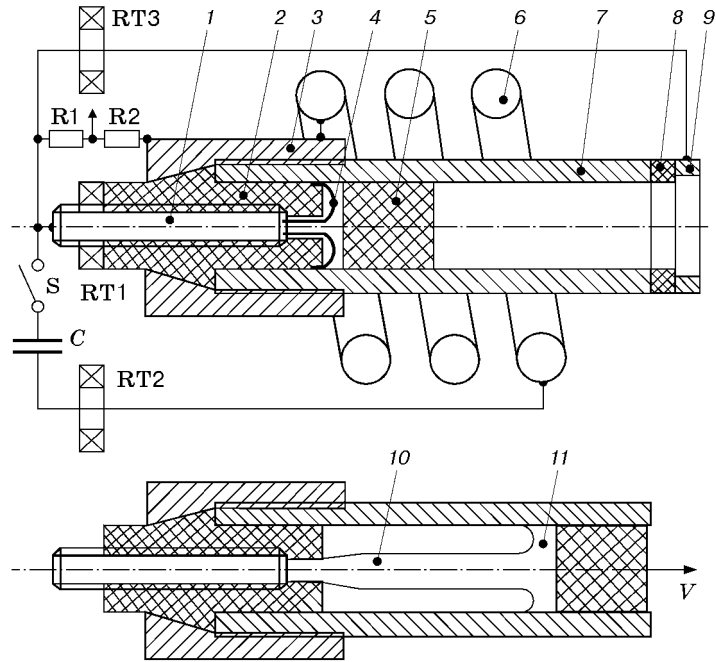


Fig. 1. Diagram of the hybrid electromagnetic accelerating system: central electrode (1), insulator with a gas-generating channel (2), pinch accelerator housing (3), electrically exploding conductors (4), projectile (5), solenoid (6), barrel electrode (7), insulator (8), auxiliary electrode (9), plasma cord (pinch) (10), plasma bridge (armature) (11), electrical switch (S), capacitive energy storage (C), Rogowski transformers (RT1, RT2, and RT3), and the low-inductance resistors of the ohmic voltage divider (R1 and R2).

Existing electrothermal guns with a barrel length of about 1.5 m accelerate bodies to velocities of 2–3 km/sec with an efficiency of up to 9–10%. The further development of pinch accelerators in the direction of activating electrodynamics was discontinued because of the instability of the plasma structure. However, even in a classical pinch accelerator, a plasma structure can be formed, compacted, and maintained dynamically in a stable state by the magnetic field of the intrinsic current so that the plasma can travel a distance of 100–150 mm or more along the accelerator channel [7]. This is indicated by the length of the continuous plasma-erosive trail on the wall of the accelerator channel and results of high-speed photography of the process at the barrel edge of a classical pinch accelerator. Hence, a considerable increase in the kinetic parameters of pinch accelerators can be expected when taking additional measures on stabilization of the stable state of the plasma structure. A stabilizing factor is the magnetic field of the inductor solenoid (see Fig. 1).

Experiments on optimization of the proposed scheme were performed for a storage capacitance of $C = 48 \cdot 10^{-3}$ F, a discharge circuit inductance of $L \approx 10^{-6}$ H (including a solenoid inductance of approximately $0.6 \cdot 10^{-6}$ H) on a device with the following structural parameters: barrel length $l_b \leq 1$ m, barrel diameter $d_b = 17$ –25 mm, solenoid length $h = 100$ mm, mean diameter of the solenoid $b = 54$ mm, number of coils $N = 3.5$, and a projectile mass $m_{pr} = 0$ –12 g (for $m_{pr} = 0$, the discharge plasma was accelerated). Projectiles of a cylindrical shape were made of polyethylene, Lexan, and metal.

The electrical parameters of accelerator operation were recorded by electron oscillographs using Rogowski transformers RT1, RT2, and RT3, which produced currents i_1 , i_2 , and i_3 , respectively, and an ohmic voltage divider, which incorporated low-inductance resistors R1 and R2 and supplied interelectrode voltage U . The moment a projectile left the barrel t_2 was determined from the moment when the plasma closed the gap between the barrel edge and the auxiliary electrode. On the oscillogram of voltage (Fig. 2), this moment corresponds to the time the current i_3 arises in the shunt circuit. In some experiments, we performed high-speed photorecording of the process at the barrel edge in the absence of a shunting electrode. The en-route motion of the projectile was recorded by several contact sensors. At the end of the route, aluminum or duralumin targets were placed.

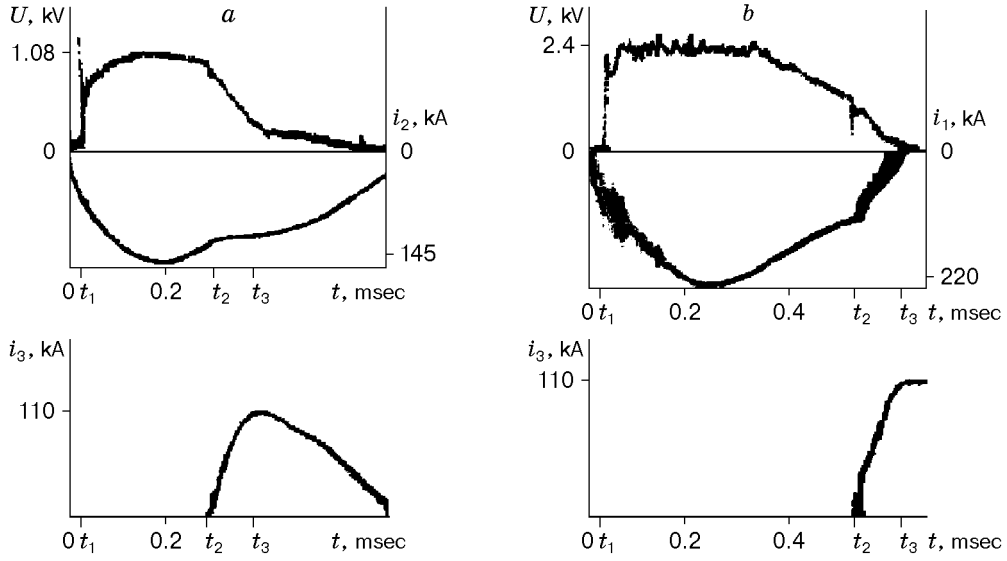


Fig. 2. Oscillograms of the electrode voltage $U(t)$, operating currents $i_1(t)$ and $i_2(t)$ and the current in the shunt circuit $i_3(t)$ during acceleration of a polyethylene projectile for $m_{pr} = 3.5$ g, $l_b = 340$ mm, $d_b = 17$ mm, and $U_{ch} = 1.75$ kV (a) and compound projectile for $m_{pr} = 80$ g (20 g Lexan and 60 g steel), $l_b = 340$ mm, $d_b = 25$ mm, and $U_{ch} = 3.5$ kV (b).

TABLE 1

Experiment number	Experimental conditions	i_m , kA	U_m , kV	W , kJ	V , km/sec	W_k , kJ	η , %
1	Pinch accelerator without an induction system. The inductor is coupled into the discharge circuit	200	0.375	25.3	0.60	1.62	6.40
2	Accelerator with an inductor. The top of the central electrode is outside the region encompassed by the inductor	200	0.380	23.0	0.28	0.36	1.57
3	The beginning of the barrel and top of the central electrode are in the plane of the first turn of the inductor. The vectors \mathbf{V} and \mathbf{H}_Z have opposite directions	192	0.513	31.5	0.70	2.21	7.02
4	The beginning of the barrel and the top of the central electrode are in the plane of the first turn of the inductor. The vectors \mathbf{V} and \mathbf{H}_Z have the same direction	188	0.630	36.5	0.81	2.94	8.05

At the initial stage of the studies, some theoretically predicted conditions necessary for the use of an auxiliary induction system were confirmed experimentally: 1) to prevent the “magnetic mirror” effect — deceleration of the current-carrying plasma structure by the edge field of the solenoid — the possible region of plasma formation and the beginning of the barrel must be placed in a plane that passes through the middle of the first turn [1]; 2) the direction of the solenoid field vector \mathbf{H}_Z , and hence, the direction of the plasma–field dipole interaction force must coincide with the direction of acceleration [8]. This follows from results of experiments on acceleration of polyethylene projectiles with a mass of 9 g (barrel length 300 mm, barrel diameter 20 mm, storage charging voltage $U_{ch} = 2$ kV) without use of a gas-generating channel in polyethylene insulator at the top of the central electrode, which are given in Table 1 [i_m is the amplitude of

TABLE 2

Experiment number	$l_{\text{m.b.}}$, mm	i_m , kA	W , kJ	V , km/sec	W_k , kJ	η , %
1	0	210	60	1.40	3.43	5.7
2	40	200	56	1.65	4.67	8.5
3	190	180	58	2.00	7.00	12.0
4	360	160	38	2.27	9.02	23.7

the accelerator operating current, U_m is the maximum electrode voltage, $W = \int_{t_1}^{t_2} U(t)i_1(t) dt$ is the energy supplied to the accelerator, V is the muzzle velocity of the projectile, $W_k = m_{\text{pr}}V^2/2$ is the kinetic energy at the barrel edge, and $\eta = (W_k/W) \cdot 100\%$ is the efficiency of conversion of the input energy to kinetic energy].

The results of experiment No. 2 (Table 1) show that with artificial removal of the top of the central electrode from the zone encompassed by the solenoid, the edge field of the solenoid prevents the current-carrying plasma structure from penetrating into the depth of the accelerating channel, which is indicated by the absence of a plasma-erosive trail on its wall. This leads to a twofold decrease in the acceleration velocity compared to the velocities attained on a classical pinch accelerator without an induction system (experiment No. 1 in Table 1). The effect of the auxiliary induction system and condition 2 can be seen from the results of experiment Nos. 3 and 4 (Table 1). In particular, irrespective of the direction of the solenoidal field vector \mathbf{H}_Z , the kinetic parameters of the system increase considerably, which is explained by stabilization of the Z -pinch high-current discharge plasma structure, and, accordingly, by establishment of better conditions for performance of useful work by the conduction electrodynamic forces. When the directions of the vectors \mathbf{V} and \mathbf{H}_Z coincide (experiment No. 4 in Table 1), the increase in final velocity and energy conversion efficiency is more considerable. The use of a gas-generating channel in polyethylene insulator at the top of the central electrode 5 mm long and 6 mm in diameter increased the initial acceleration dynamics, and with satisfaction of the two indicated conditions, a velocity of $V = 1.4$ km/sec is attained with an energy conversion efficiency of 15.8%. The complete hybrid system ensures more than a twofold increase in the velocity and acceleration efficiency compared to the classical pinch accelerator under the same current supply conditions and main design parameters. The final result of operation of the pinch accelerator with the auxiliary induction system is determined by the combined contribution of the electroexplosive and electrothermal mechanisms (15%) and the induction and conduction mechanisms (10 and 75%, respectively).

The analogy between the mechanism of operation of electrodynamic forces in the system considered and a coaxial railgun, where a self-elongating plasma cord (pinch) acts as the central directive force is confirmed by a series of experiments, whose results are shown in Table 2. The length of the conducting metal part of the barrel $l_{\text{m.b.}}$ was varied with its unchanged overall length of 360 mm. The metal part was supplemented by a dielectric fiberglass part. Polyethylene projectiles with a mass of $m_{\text{pr}} = 3.5$ g were accelerated (barrel diameter $d_b = 17$ mm, charging voltage $U_{\text{ch}} = 1.75$ kV). The experiments showed that for zero length of the metal part, the presence or absence of an inductor does not influence the result of the shot. The results of experiments with a dielectric barrel channel confirm the assumption of the important role of the electroexplosive and electrothermal mechanisms in the acceleration process and refute the assumption of a purely inductive mechanism for acceleration of a plasma bunch. An analysis of the results presented in Table 2 shows that the muzzle velocity and the energy conversion efficiency increase with increase in $l_{\text{m.b.}}$. This can be explained only assuming the existence of a stable self-elongating plasma cord (Z -pinch) with a current-carrying plasma bridge moving under the action of the Ampere force. The estimate of the contribution from each of the above-mentioned mechanisms obtained from the experimental results presented in Table 2 agrees with that given above. Similar results were obtained on a pinch accelerator with explosive switching of the operating current and preacceleration of the projectile [9]. In this case, an additional factor of plasma compaction is the flow of the detonation products of the explosive.

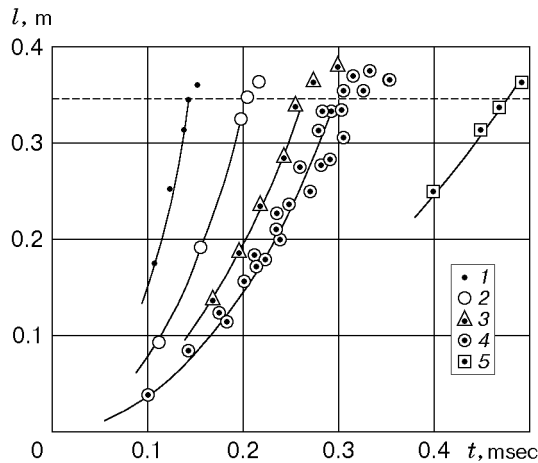


Fig. 3. Time the projectile leaves the barrel versus barrel length ($d_b = 17$ mm and $U_{ch} = 1.75$ kV) for $m_{pr} = 0$ (plasma) (1), 1 (2), 2 (3), 3.5 (4), and 12 g (5).

In the system considered, the metal wall of the barrel screens the accelerating channel. The auxiliary magnetic field in it is a superposition of the solenoidal field and the field of the transverse current induced in the barrel wall. By varying the magnitude of the transverse conductivity of the barrel wall and combining magnetic and nonmagnetic metals in the pinch-accelerator design, one can specify the law of variation in the auxiliary magnetic field in the accelerating channel. Optimization of the design allows one to produce a short pause during which there is no field in the region of formation of the plasma structure and to ensure the subsequent monotonic increase in the field during the entire acceleration time, even with decrease in the operating current. At the initial stage, the rate of rotation of the plasma bridge by the azimuthal field is reduced to a minimum.

Under the indicated conditions, the acceleration dynamics of the plasma structure and a projectile was studied experimentally for the hybrid accelerating system. The barrel length of the pinch accelerator was varied from 50 mm to 1 m. With reliable recording of the moment the plasma leaves the barrel (following the projectile), each shot gave one point on the curve of the law of motion in the barrel. It is possible to examine the effect of the barrel length on the final velocity of the projectile and to solve two practical problems: 1) cutoff of the current pulse tail; 2) switching of the electric power supply for possible use at the subsequent acceleration stage.

Figure 2 gives oscillograms of the accelerator electrode voltage, operating current, and the shunt circuit current. The reference time corresponds to the moment of closure of the switch S (see Fig. 1). The time t_1 corresponds to the electric explosion of the conductors and the beginning of operation of the accelerator, the time t_2 corresponds to closure of the shunting gap and exit of the projectile from the barrel, and the time t_3 corresponds to complete diversion of the current to the shunt circuit. An analysis of the oscillograms of all experiments shows that the spread of the voltage and current strength and the difference in the energy supplied to the load are not more than 5%.

The experimental dependence of the time the projectile leaves the barrel versus the barrel length is shown in Fig. 3. It is evident that on a barrel segment with a length of 50–340 mm, the acceleration characteristics are close to the law of motion with constant acceleration a :

$$l = at^2/2. \quad (1)$$

This agrees with the data of [3, 4, 6] for an acceleration segment of small length, on which the current-carrying plasma structure can pass into the depth of the barrel in a conventional pinch accelerator. The law of motion (1) holds over the entire range of mass of the projectiles used. The dependence $l(t)$ was studied most comprehensively for a projectile mass of 3.5 g. For a barrel length of more than 340 mm, the experimental

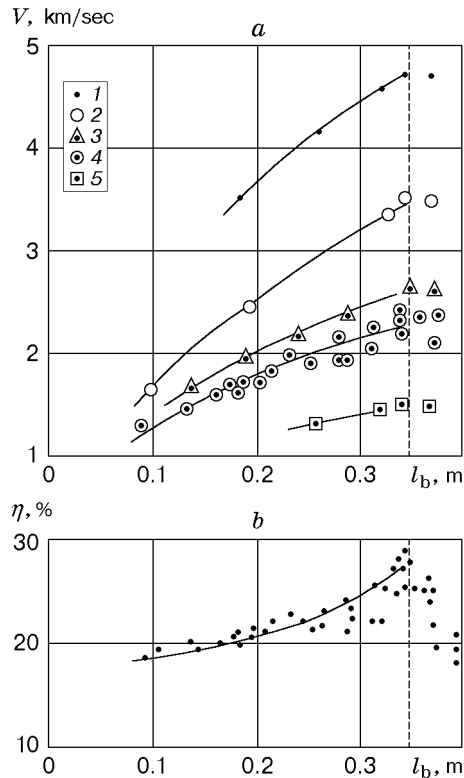


Fig. 4. Muzzle velocity (a) and efficiency of conversion of the input energy to kinetic energy (b) versus the barrel length (the notation is the same as in Fig. 3).

points are deflected to the right not only from the curve corresponding to relation (1) but also from the straight line corresponding to a linear relation. Delay of the breakdown of the shunting gap is observed. For a barrel length of more than 340–350 mm, the velocity practically does not vary at the same distance from its edge.

In all experiments, the barrel was cut after shot. An analysis of the surface of the accelerating channel shows that for any barrel length there is a relation between the velocity and the length of the continuous plasma-erosive trail. In the experiments performed, the length of this trail did not exceed 340–350 mm even when the barrel length was much greater barrel. This relation is the same for both a classical pinch accelerator and an accelerator with an induction system. We note that the plasma-erosive trail is not suddenly interrupted but is divided into separate “tongues,” which are spalled from the barrel surface that is not affected by erosion. This structure suggests that the motion of the current-carrying plasma bridge (armature) ceases, and separate “tongues” result from spread of the molten metal.

From the aforesaid it follows that the auxiliary magnetic field ensures a stable state of the current-carrying plasma structure on an accelerating channel segment whose length exceeds the solenoid length by approximately 250 mm. On this “active” segment of the barrel, the plasma bridge and the projectile are launched with a nearly constant acceleration.

Guaranteed breakdown of the shunting gap occurs when the current-carrying plasma escapes from the barrel. When the barrel length is greater than the length of the “active” segment, the plasma that leaves the barrel does not carry current, and, therefore, breakdown delays or does not occur.

Thus, on a barrel length smaller than or equal to the length of the “active segment,” the muzzle velocity is given by the formula

$$V = 2l_b/t_{12}, \quad (2)$$

where $t_{12} = t_2 - t_1$ is the acceleration time.

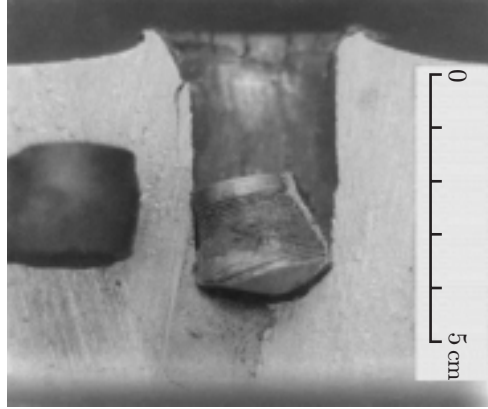


Fig. 5. Crater in an Duralumin target with a steel impactor with a mass of 60 g and a preserved Lexan plate with a mass of 20 g for a collision velocity of 1 km/sec.

Figure 4a gives the muzzle velocity and the approximating curves 1–5 calculated from formula (2); the average accelerations for the projectile masses used are equal to $3.3 \cdot 10^7$, $1.32 \cdot 10^7$, $0.96 \cdot 10^7$, $0.77 \cdot 10^7$, and $0.32 \cdot 10^7$ m/sec², respectively. Figure 4b shows the efficiency η of conversion of input energy to kinetic energy versus the barrel length for projectile masses of 1–12 g. The curve is drawn by the experimental points obtained for a projectile mass of 3.5 g. From the experimental results it follows that with increase in the barrel length to 340 mm, the increase in the muzzle velocity is accompanied by an increase in the efficiency of conversion of the input energy. Under optimal conditions, the hybrid accelerating system ensures an efficiency of 25–29%, irrespective of the projectile mass, the energy supplied to the accelerator, and the muzzle velocity of the projectile. For electrothermal guns, the efficiency decreases sharply for $V > 2$ km/sec [10].

Measurements show a decrease in the en-route projectile velocity, which agrees with the law of exponential decrease in velocity [11–13]. In the present work, this was supported experimentally by observations of several contact sensors and also by high-speed photography of the process at the barrel edge under normal conditions and using a transparent Plexiglas nozzle at the barrel edge. The projectile velocity in a transparent nozzle 40 mm long recorded by an optical method practically coincides with that calculated from formula (2) using the law of exponential decrease.

In acceleration of heavy projectiles with a mass of several tens of grams, the decrease in velocity at distances less than 1.5 m is very small. Therefore, all methods for determining the muzzle velocity give close values, which differ by not more than 10%. Figures 2 and 5 give the results of a shot from a more powerful hybrid system compared with that used for acceleration of projectile masses of 1–12 g. For acceleration of a projectile mass of 80 g a velocity of 1 km/sec was recorded, and the muzzle velocity calculated from formula (2) is equal to 1.05 km/sec. The energy conversion efficiency was 20%. This value is smaller than that for acceleration of light projectiles because of the insufficient amount of the capacitive storage energy and transition of the system to an acceleration regime with decreasing current (see Fig. 2b). Figure 5 gives a photograph of a crater in a duralumin target with a steel impactor with a mass of 60 g and a practically preserved Lexan plate with a mass of 20 g. The decrease in the projectile mass to 40.2 g ensured its acceleration in the regime of nondecreasing current to a final velocity of 1.3 km/sec with an efficiency of energy conversion of 27.8%.

The maximum kinetic parameters of acceleration obtained in the present work are presented in Fig. 6 as a curve of the muzzle velocity versus projectile mass. Each curve is drawn by experimental points obtained for the same parameters of the accelerating system and the same parameters of the current supply, indicated in the table of Fig. 6, where the test numbers correspond to the curve numbers. In all cases, the efficiency of less than 20% with increase in the projectile mass is due to the transition of the system to the acceleration regime with decreasing current. Acceleration with nondecreasing current was not achieved because of the

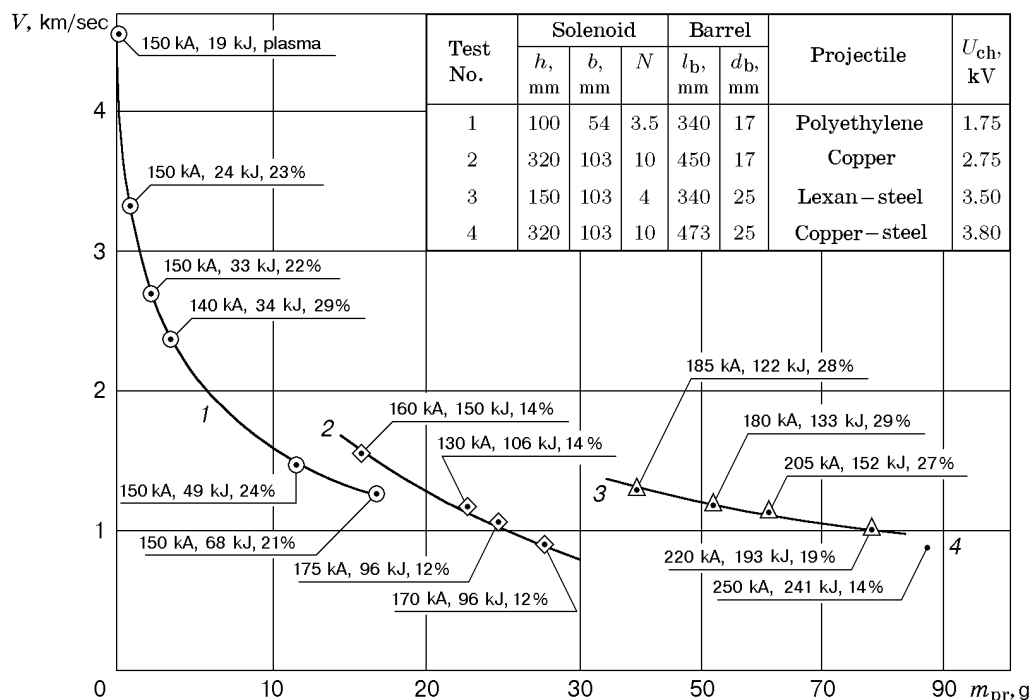


Fig. 6. Muzzle velocity of the projectile versus projectile mass (for each point, the maximum current, input energy, and efficiency of energy conversion are indicated).

limited possibilities of the available primary energetics. The results represented by curves 2 and 4 are obtained using a 10-turn solenoid with a length of 320 mm. A distinctive feature of the acceleration using this solenoid is that the plasma-erosive trail covers the entire length of the barrel, which suggests that the plasma structure is in a stable state on a segment with a length of more than 450 mm. Hence, one might expect to attain higher velocities by increasing the primary energetics.

The oscillograms of the electrode voltage and currents presented in the paper show that the system effectively diverts the current to the parallel circuit. These conditions ensure cutoff of the current pulse tail, which can be used to switch the current supply to the second acceleration stage without using an auxiliary switcher.

It should be noted that the specific energy of experimental specimens of the accelerating system is about 1–5 kJ neglecting the primary storage.

The main result of the present work is the proof that the optimized hybrid electromagnetic accelerating system ensures high, nearly constant efficiency over a rather wide range of projectile masses for currents of 150–200 kA. As a result, for projectiles masses of about 0.1 kg and more, one might expect acceleration velocities of 2–3 km/sec with an energy conversion efficiency of 25–30%. The system can be used separately and as the first stage of a more powerful system, ensuring switching of the current supply to the next acceleration stage.

This work was supported by the Ministry of Education of the Russian Federation (Grant No. 97-12-9.1-1).

REFERENCES

1. A. A. Sivkov, "Coaxial accelerator," Patent of the Russian Federation No. 2119140 RF, 6 F 41 V 6/00, Appl. 06.24.97; Publ. 09.20.98, Bull. No. 26.
2. R. A. Burden, I. W. Gray, and C. M. Oxley, "Explosive foil injection (EFI) preaccelerator for electromagnetic launchers," *IEEE Trans. Magn.*, **25**, No. 1, 107–110 (1989).

3. A. A. Sivkov, "Sivkov's coaxial accelerator," Patent of the Russian Federation No. 2150652 RF, 7 F 41 V 6/00, Appl. 02.24.99; Publ. 06.10.00, Bull. No. 16.
4. J. G. H. Salge, Th. H. G. G. Weise, U. E. Braunsberger, et al., "Mass acceleration by plasma pulses," *IEEE Trans. Magn.*, **25**, No. 1, 495–499 (1989).
5. A. Loeb and Z. Kaplan, "A theoretical model for the physical processes in the confined high pressure discharges of electrothermal launchers," *ibid.*, pp. 342–346.
6. M. D. Driga, M. W. Ingram, and W. F. Weldon, "Electrothermal accelerators: The power conditioning point of view," *ibid.*, pp. 147–152.
7. V. I. Modzolevskii, "Plasma current shell in coaxial accelerators of the microsecond range," in: *Proc. of the 1st All-Union Seminar on the Dynamics of a High-Current Electric Arc in a Magnetic Field* (Novosibirsk, April 10–13, 1990), Inst. of Thermal Physics, Sib. Div., Russian Acad. of Sci., Novosibirsk (1990), pp. 220–251.
8. H. Knoepfel, *Pulsed High Magnetic Fields*, North Holland, Amsterdam–London (1970).
9. A. A. Sivkov, "Explosive switching in electrodynamic accelerators of masses," *Izv. Vyssh. Uchebn. Zaved., Fiz.*, No. 4, 164–172 (1996).
10. M. Guillemot, A. Nicolas, and M. Roche, "Projectile launching by an electrothermal gun," *IEEE Trans. Magn.*, **25**, No. 1, 207–209 (1989).
11. N. A. Zlotin, A. P. Krasil'shchikov, G. I. Mishin, and N. N. Popov, *Ballistic Facilities and Their Use in Experimental Studies* [in Russian], Nauka, Moscow (1974).
12. É. M. Drobyshevskii, B. G. Zhukov, and V. A. Sakharov, "Measurements of high velocities of projectiles with small geometrical dimensions," *Pis'ma Zh. Tekh. Fiz.*, **19**, No. 17, 45–48 (1993).
13. D. A. Andreev, A. A. Bogomaz, F. G. Rutberg, and A. N. Shakirov, "Acceleration of projectiles with small masses by the a Z-pinch high-current discharge at high initial density," *Zh. Tekh. Fiz.*, **63**, No. 1, 203–205 (1993).